On the Mechanism of Sulfur Dioxide Oxidation in Cloud Drops

A. N. Yermakov[a], **, A. E. Aloyan[b], V. O. Arutyunyan[b], and G. B. Pronchev[a], *

[a] *Institute of Energy Problems of Chemical Physics, Russian Academy of Sciences, Moscow, 119334 Russia*
[b] *Marchuk Institute of Numerical Mathematics, Russian Academy of Sciences, Moscow, 119333 Russia*
e-mail: polclouds@yandex.ru
**e-mail: ezmakr2010@yandex.ru*

Abstract—Data from field experiments on the dynamics of SO_2 oxidation in cloud droplets are presented. The rapid experimentally observed oxidation of SO_2 by molecular oxygen is attributed here to the catalytic action of a pair of manganese and iron ions in droplets. Their effect, inhomogeneous in the drop-size distribution and attributed in experiments only to the leaching of ions of these metals from coarse particles of mineral aerosol, is also caused by the transition of the oxidation reaction into the branching mode. The results indicate that the branched regime of catalytic oxidation of SO_2 detected in cloud droplets should be considered a new and significant source of sulfates in the atmosphere. This process must be taken into account when considering both the budget of sulfates in the global atmosphere and their impact on the climate.

INTRODUCTION

Sulfates in the global atmosphere directly and indirectly impact the radiation regime of the atmosphere and climate (Kulmala et al., 2000; Andreae et al., 2005). More than a half of them are formed in the process of sulfur dioxide oxidation in the atmosphere (in particular, in the droplet phase). These heterophase intracloud reactions of sulfur dioxide oxidation play an important part in the self-purification of the atmosphere (acid rains, etc.) (Seinfeld and Pandis, 2016). The formation of sulfates in cloud droplets is associated mainly with the H_2O_2 and O_3 uptake from the air (Seinfeld and Pandis, 2016). Along with this, dark (nonphotochemical) mechanisms of sulfate formation in droplets are also considered (Warneck et al., 1996; Zheng et al., 2015; Cheng et al., 2016; Wang et al., 2016; Xie et al., 2019). They include understudied catalytical routes of SO_2 oxidation by molecular oxygen in the presence of transition metal (TM) ions (Alexander et al., 2009). The contribution of these processes to the formation of sulfates in the global atmosphere remains unclear, however. Their underestimation in the global SO_2 distribution in the atmosphere was reported in (Feichter et al., 1996, Fomba et al., 2013) and other works. In opposition to this, in (Berglen, 2004), it was reported with the use of the OsloCTM2 model that the time of SO_2 oxidation in catalytic processes amounted to about 50 days, which indicated their insignificant role in the atmosphere. In recent years, reports about episodes of the anomalously rapid production of sulfates generated in catalytic processes (tens of $\mu g\ m^{-3}\ h^{-1}$) in atmospheric aerosol became more frequent (Zheng et al., 2015; Cheng et al., 2016; Wang et al., 2016; Xie et al., 2019). In (Alexander et al., 2009), their formation in the global atmosphere was considered using the GEOS-Chem three-dimensional model involving laboratory modeling data on kinetics of catalytic processes in solutions (in what follows, in bulk conditions/experiments). For TM ions in (Alexander et al., 2009), the most active ones in their series were considered: Mn^{2+} and Fe^{3+} ions (Coughanowr and Krause, 1965; Ibusuki and Takeuchi, 1987; Martin and Good, 1991; Grgić et al., 1991; Berglund et al., 1993). However, the calculated concentrations of SO_2 and sulfates in (Alexander et al., 2009) turned out to be several times higher when compared to monitoring data (Harris et al., 2013). We emphasize that the mechanism of catalytic transformations of SO_2 in droplets was not considered in an explicit form in GEOS-Chem, WRF-Chem (Wang et al., 2016; Grell et al., 2005), or in other atmospheric models. Instead of this, empirical expressions obtained for rates of catalytic reactions in bulk experiments at separate (w_{Mn}, w_{Fe}) or joint (w_{Mn_Fe}, mol $L^{-1}\ s^{-1}$) finding of ions of these metals were used (Ibusuki and Takeuchi, 1987). Such an approach made it possible to reduce computational resources, but meets serious objections (Ermakov and Purmal, 2002; Ermakov, 2022). The possibility that the catalytic action of TM ions can be

activated by an uptake of H_2O_2 from air and, in the daytime, OH and HO_2 radicals, or by the absorption of the Sun's radiation was also left out of accounts (Warneck et al., 1996; Herrmann et al., 2000). The aim of this work is, based on results of our investigations of the mechanism of catalytic reactions with the participation of TM ions (Ermakov and Purmal, 2002; Eremina et al., 2017) and using data of field experiments (Laj et al., 1997, Sedlak et al., 1997; Harris et al., 2013), reveal features of the dynamics of such processes in cloud droplets in the atmosphere.

PRELIMINARIES

The predominant participation of processes in the droplet phase with the participation of hydrogen peroxide and ozone in oxidation of sulfur dioxide (up to ≈80%) is indicated by the results of 3D modeling (OsloCTM2, NCAR CCM3, GLOMAP, and others) of the global distribution of sulfur dioxide in the atmosphere. The participation of hydrogen peroxide (H_2O_2) in sulfur dioxide oxidation in cloud droplets is directly pointed by data of the Great Dun Fell campaign (the United Kingdom) (Laj et al., 1997; Sedlak et al., 1997). In those experiments, it was reported about the correlation between the increment of the sulfate and dissolved H_2O_2 concentrations normalized to the concentration of the tracer (Na_{aq}^+ ions). At the same time, it was also noted that concentrations of valence forms of iron ions (Fe^{2+}/Fe^{3+}) in droplets varied with the compositional range of air or changes in the time of day (insolation level), which indirectly says about the participation of metal ions in catalytic transformations of SO_2 (Behra et al., 1990).

The involvement of TM ions in the formation of sulfates in the atmosphere is directly indicated by monitoring data on the isotopic composition of atomic oxygen ($\Delta^{17}O$) in them in hardly deliquesced aerosol particles (McCabe et al., 2006). Data of field monitoring experiments on the isotopic composition of sulfur atoms ($\Delta^{34}S$) in sulfur dioxide and sulfates in cloud droplets in the background region in the Febuko and Hill Cap Cloud Thuringia campaigns (HCCT-2001 and HCCT-2010) also serve as a corroboration (Harris et al., 2013). Southwest winds in mountains of Thuringian Forest, passing through three weather stations, cross the mountain system from southeast to northwest, which is often accompanied by the formation of orographic clouds over Schmücke (937 m above sea level). The Goldlauter upwind station (605 m above sea level) is located about 3 km southwest of the Schmücke station; the downwind Gehlberg station (732 m above sea level) is about 3 km northeast of Schmücke. The samples for the analysis of sulfur isotopes in HCCT-2010 were taken both for cases of cloud appearance and in the cloudless period. The HCCT-2010 data directly indicate that the main part

of sulfates in cloud droplets in some episodes is formed just with the participation of TMs.

Note that monitoring of the isotopic composition of reagents and products with the aim of revealing the nature of sulfate formation in the atmosphere has a history. For example, in (Gröner and Hoppe, 2006; Winterholler, 2008), it was reported about differences in the content of ^{34}S in SO_2 and sulfates in air. They indicate isotopic fractionation in the process of conversion $SO_2 \rightarrow SO_4^{2-}$ in the atmosphere. These differences are discernible when comparing data about the isotopic composition of sulfur dioxide and sulfates, both in background and in urbanized regions. The isotopic fractionation in the process of conversion $SO_2 \rightarrow SO_4^{2-}$ is also observed in data of laboratory experiments. For example, when SO_2 is oxidized in solutions containing H_2O_2 or O_3, enrichment of the sulfate with the ^{34}S isotope is observed; the isotopic composition of sulfur dioxide that passed through the solution, on the contrary, is enriched with the light ^{32}S isotope. In contrast to this, when SO_2 is oxidized by molecular oxygen, the formation of sulfates depleted in the ^{34}S isotope is observed (Harris et al., 2012a). In this process, SO_2 is enriched with the ^{34}S isotope, which allows one also to differentiate the channels of sulfur dioxide oxidation in cloud droplets. For example, at $T \approx 293$ K, the changes found in laboratory conditions in the relation between the contents of the heavy ^{34}S and light ^{32}S isotopes ($\Delta^{34}S$) when sulfur dioxide was oxidized by H_2O_2, O_3, and molecular oxygen, according to (Harris et al., 2012a), were as follows: $\alpha_{aq\_H_2O_2} \approx \alpha_{aq\_O_3} = 1.0167$ and $\alpha_{aq\_R} = 0.9894$, respectively. Here, $_R$ serves as a notation for the process of SO_2 oxidation by molecular oxygen with the participation of free radicals (R).

MONITORING DATA AND THEIR ANALYSIS

H_2O_2 and O_3 in Sulfur Dioxide Oxidation

The observation of $\Delta^{34}S$ when the SO_2 impurity (≈0.1 ppb) passes a cloud from the upwind to the downwind side showed that the participation of H_2O_2 and O_3 in oxidation of sulfur dioxide predominate only in the first (nighttime) episode (Harris et al., 2013). In the second nighttime episode (FCE 11.2) and third episode (FCE 11.3), combining the night and day, data of $\Delta^{34}S$ monitoring in sulfur dioxide evidence about the decisive participation of molecular oxygen in oxidation of the SO_2 impurity (Harris et al., 2013). Below, we consider data of the nighttime episode (FCE 11.2). Choosing them excludes from the consideration the influence of processes of daytime OH radical uptake from gas on the depth of SO_2 oxidation, as well as processes of their generation during photolysis in droplets of H_2O_2 and others.

The time-averaged ($\approx$7 h) change in the isotopic composition of sulfur atoms in the sulfur dioxide impurity that passed ($_{dw}$) through the cloud at $T \approx 280$ K and relative air humidity close to 100% corrected for dilution of air masses between control points (experiments with the SF_6 tracer) amounted to $\Delta^{34}S_{dw} = 0.04558$. At the same time, monitoring of $\Delta^{34}S$ in sulfur dioxide coming from the upwind side ($_{upw}$) yields $\Delta^{34}S_{upw} = 0.044$. This is an indication of the enrichment by the heavy ^{34}S isotope in the fraction of the sulfur dioxide impurity that passed through the cloud (McCabe et al., 2006; Alexander et al., 2009); the enrichment demonstrates the participation of molecular oxygen in SO_2 oxidation in droplets. Indeed, the expected change in $\Delta^{34}S$ under the same conditions when sulfur dioxide is oxidized by hydrogen peroxide ($\approx$0.01 ppb (Harris et al., 2013)) would be accompanied by $\Delta^{34}S_{dw\_H_2O_2} = \Delta^{34}S_{upw}$ $\exp((\alpha_{H_2O_2}-1)\ln(f)) = 0.04257$ (McCabe et al., 2006; Alexander et al., 2009), which is lower than in SO_2 coming from the upwind side. A comparison of $\Delta^{34}S_{dw}$ and $\Delta^{34}S_{dw\_H_2O_2}$ shows that hydrogen peroxide in fact does not participate in sulfur dioxide oxidation in the nighttime episode FCE 11.2. However, the causes of H_2O_2 inertness in the episode FCE 11.2 remain unclear in view of high solubility of hydrogen peroxide and its pronounced reactive capacity in regard to components of SO_2 dissolved in droplets (Herrmann et al., 2000). Ozone uptaken from air also does not participate in SO_2 oxidation in this episode. This is caused by low concentrations of the SO_3^{2-} anion at pH 3.8—the dissolved sulfur dioxide component that is active for ozone, as well as by low solubility of O_3 (Herrmann et al., 2000). Summarizing, one may state that sulfur dioxide conversion detected by the change in the isotope composition in droplets of the nighttime cloud (FCE-11.2) is implemented exclusively by molecular oxygen and with the participation of free radicals in the process.

Insignificant Role of NO₃

Along with the generation of the latter in processes with the participation of iron ions and components of dissolved SO_2 (van Eldik et al., 1992), one should also reckon with the uptake of nighttime NO_3 radicals and gaseous molecules of H_2O_2 by droplets. The low reactive capacity of NO_3 in regard to SO_2, CO, H_2S, etc., differs them from daytime OH radicals. At night time, [NO_3], even over the background area, can reach values which are two or three orders higher than [OH] in the daytime ($\approx 2 \times 10^6$ cm^{-3} (Mauldin et al., 1997; Herrmann et al., 2000)). The reaction of electron transfer from HSO_3^- (a component of dissolved SO_2) to NO_3 ($NO_3 + HSO_3^- \rightarrow NO_3^- + SO_3^- + H^+$) (Berd-

nikov and Bazhin, 1970), on the contrary, is fast, which indicates a potentially fast initiation in droplets. To estimate the NO_3 participation in this process, it is necessary, however, to reckon with the competition of NO_3 formation/consumption in the gas and with the process of their drag to the droplet phase. The key factor is the competition of two processes: the decomposition of particles $N_2O_{5(g)}$ ($N_2O_{5(g)} + M \rightarrow NO_{3(g)} + NO_{2(g)}$, τ_d) and their dissolution (τ_{dis}) terminating with rapid hydrolysis: $N_2O_{5(aq)} + H_2O \rightarrow NO_{2(aq)}^- + NO_{3(aq)}^- + 2H_{(aq)}^+$. Here, $_{(g)}$ and $_{(aq)}$ show that the considered components belong to the gas and condensed phases. For small droplets, the dissolution of $N_2O_{5(g)}$, i.e., the "useless" death of $NO_{3(g)}$, turns out to be prevailing. The following droplet size is critical: $r_{cr} \geq 3\alpha \varpi L/4 \tau_{dis} \geq 4$ μm. Here, α is the accommodation coefficient (3.7×10^{-3} (Herrmann et al., 2000)); ϖ is the average thermal velocity of $N_2O_{5(g)}$ molecules, cm/s; and L is the volume content of condensed moisture in the air, cm^3(aq)/cm^3(gas). In this regard, we note that studying samples of condensation nuclei and condensed moisture in the cloud with the use of scanning electron microscopy, nanoscale secondary ion mass spectrometry, and other methods in (Harris et al., 2013) showed that catalytic oxidation occurred exclusively on deliquesced particles of coarsely dispersed mineral aerosol of natural origin. It turned out that these particles served as sources of TM ions in droplets in the FCE-11.2 episode, which was also corroborated by the results of recent independent observations of their leaching (Harris et al., 2012b). However, since the fraction of the condensed moisture content on these particles ($\geq$3 μm) does not exceed 1% of the total water content of the cloud (Harris et al., 2013) (see the solid line *1* in Fig. 1), the role of NO_3 in the initiation of the catalytic reaction of SO_2 oxidation seems negligible.

Decisive Role of Molecular Oxygen in the Formation of Sulfates

Hydrogen peroxide molecules uptaken from the air also can participate in acceleration of catalytic conversion $SO_2 \rightarrow SO_4^{2-}$ in the cloud, which also favors the increase in the initiation rate of the catalytic reaction ($H_2O_2 + Fe^{2+} \rightarrow OH$ (Herrmann et al., 2000)). However, the data of our calculations with the use of the reduced (shortened) mechanism (the CHEMWG model (Laj et al., 1997)) did not corroborate this hypothesis. Their results showed that the major part of H_2O_2 in droplets is consumed in the reaction with components of dissolved SO_2, and the reaction $HSO_3^- + Fe^{2+} \rightarrow SO_4^-$ ((9), see Table 1) serves as the main channel of radical generation (Herrmann et al., 2000). This result also agrees with data of independent calculations of the dynamics of atmospheric chemical

reactions in the background area (Tilgner et al., 2013) using the full CAPRAM 3.0i mechanism, but it contradicts the data presented above about the nonparticipation of H_2O_2 in SO_2 oxidation in FCE-11.2 (Harris et al., 2013). Summarizing, we come to the conclusion that the decisive role in the formation of sulfates in the nighttime episode FCE-11.2 belongs to reactions of radicals and molecular oxygen in droplets and that the use of the quantity α_{aq_R} for calculations of $\Delta^{34}S$ is correct. Turning to the increase in $\Delta^{34}S$ in sulfur dioxide observed in this episode FCE-11.2, we have $\Delta^{34}S_{dw\_R} = \Delta^{34}S_{upw} \exp((\alpha_{aq\_Fe} - 1) \ln(f)) = 0.045$. Here, according to data (Harris et al., 2012a), it is taken that $\alpha_{aq\_R} = \alpha_{aq\_Fe} = 0.9894$ and f = 0.13 (Harris et al., 2013). The quantity $\Delta^{34}S_{dw\_R}$ calculated here agrees reasonably well with data of field measurements (0.0458) and indicates an almost 100% conversion $SO_2 \to SO_4^{2-}$ in the cloud along the catalytic route with the participation of molecular oxygen and transition metal ions.

Fig. 1. Effect of the volume fraction of moisture in particles of an orographic cloud at pH $\approx$ 3.8, T = 280 K, and $P_{SO_2} \approx 0.1$ ppb (the HCCT-2010 campaign) on the relation of concentrations of Mn^{2+} and S(IV) ions (the left axis) and rate w_{Mn_Fe} of the catalytic reaction of sulfur dioxide oxidation in droplets (the right axis).

Estimates of the Liquid-Phase Oxidation Rate

As emphasized above, the fraction of moisture in which the catalytic reaction proceeds does not exceed 1% on deliquesced particles of coarsely dispersed mineral aerosol (see the solid line in Fig. 1). This means that the process of SO_2 oxidation on these particles should proceed very rapidly, which is supposedly corroborated by the value reported in (Harris et al., 2013) for the coefficient of reactive SO_2 uptake by droplets (γ_{SO_2} = 0.1). For the catalytic reaction rate on the gaseous phase basis by these data, we have $W_{S(VI)\_atm.} = \gamma_{SO_2}[SO_2]\varpi_{SO_2} 3L/4r$, where r is the radius of deliquesced particles and ϖ_{SO_2} is the average speed of SO_2 molecules, cm/s. Here, S(IV) $\approx SO_{2(aq)} + HSO_3^-$ is the total content (mol/L) of dissolved sulfur dioxide components at pH $\approx$ 3.8. Taking according to data of this publication $r \approx 5$ μm and $L \approx 4 \times 10^{-9}$ (4×10^{-9} m³ (aq)/m³ of air), we find L/r $\approx 8 \times 10^{-6}$ cm⁻¹ and $W_{S(VI)\_atm.} \approx 10^8$ cm⁻³ s⁻¹. For the SO_2 lifetime in the atmosphere in regard to the reactive intake by droplets, we have $\tau_{SO_2} = [SO_2]/W_{S(VI)\_atm.} \approx 70$ s. The value of τ_{SO_2} calculated in this way points to extremely high activity of Mn/Fe ions, but it turns out to be about four orders less than that taken from (Berglen et al., 2004). For the rate of the reaction in the droplet phase, according to data on γ_{SO_2} (Harris et al., 2013), we have $w_{S(VI)\_atm.\_aq} = W_{S(VI)\_atm.} 10^6/N_aL \, 10^3 \approx 7 \times 10^{-5}$ mol L⁻¹s⁻¹, where N_a is the Avogadro number and 10^6 and 10^3 are the dimension factors, cm³/m³ and L/m³. Such a high rate of liquid-phase oxidation at relatively low concentrations of Mn/Fe and low content of SO_2 raises doubts. The following is a calculation of the quantity $w_{S(VI)\_atm.\_aq}$; it
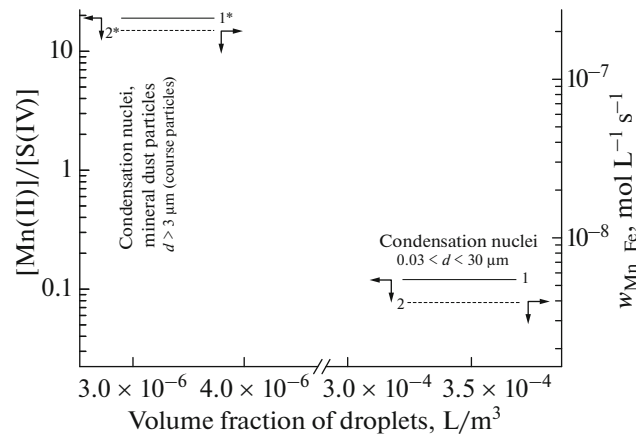
relies on the results of direct experiments on the dynamics of the catalytic reaction in bulk conditions. For this purpose, we use the known expression for the catalytic reaction rate: $w_{Mn\_Fe} = k_{Mn\_Fe}$ [S(IV)] (Ibusuki and Takeuchi, 1987). Here, $k_{Mn\_Fe} = 3.7 \times 10^7$ [Mn(II)][Fe(III)]/$(10^{-pH})^{-0.74}$ s⁻¹ is the observed reaction rate constant. The concentrations of Mn/Fe ions in droplets are found by data about their content averaged over the episode: 0.24 and 4 ng/m³, respectively. The content of condensed moisture on large particles, in accordance with (Harris et al., 2013), is taken to be equal to 1% of its total content (3.7×10^{-4} cm³/m³), i.e., $\approx 4 \times 10^{-6}$ L/m³ (see Fig. 1). At $T \approx 280$ K and pH 3.8 ($\leq$4.2 (Ibusuki and Takeuchi, 1987)), we have from this $k_{Mn\_Fe} \approx 3 \times 10^{-2}$ s⁻¹ and $w_{Mn\_Fe} = k_{Mn\_Fe}$ [S(IV)] $\approx 3 \times 10^{-9}$ mol L⁻¹ s⁻¹. The value of w_{Mn_Fe} calculated by data of bulk experiments on the gaseous phase basis is much less than the $W_{S(VI)\_atm.}$ presented above, which calls into question not only the value of the reactive coefficient of SO_2 uptake (Harris et al., 2013). The value of w_{Mn_Fe} exceeds the rate of SO_2 oxidation with the participation of hydrogen peroxide: $w_{H_2O_2} = k_{H_2O_2}[H_2O_2][HSO_3^-] \approx 10^{-9}$ mol L⁻¹ s⁻¹, although, in contradiction to what was said in (Harris et al., 2013), it indicates the potentially significant participation of hydrogen peroxide in oxidation of HSO_3^- in this episode. Here, $k_{H_2O_2} = 7.45 \times 10^7 \times 10^{-pH}$ L mol⁻¹ s⁻¹ is the rate constant of the reaction $H_2O_2 + HSO_3^-$ (Betterton and Hoffman, 1988) in the expression for $w_{H_2O_2}$, and [H_2O_2] and [HSO_3^-] are the concentrations of hydrogen peroxide and component of diluted SO_2 in cloud droplets.

Table 1. Mechanism of sulfite oxidation catalysis by manganese ions ($\mu \approx 0$)

No.	Reaction	Rate constant, L mol^{-1} s^{-1}
1	$Fe(OH)SO_3H^+ \rightarrow Fe^{2+} + SO_3^- + H_2O$	*0.2
2	$SO_3^- + O_2 \rightarrow SO_5^-$	2.5×10^9
3a	$SO_5^- + HSO_3 \rightarrow HSO_5^- + SO_3^-$	3.4×10^3
3b	$SO_5^- + HSO_3^- \rightarrow SO_4^{2-} + SO_4^- + H^+$	2×10^2
4	$SO_4^- + HSO_3^- \rightarrow SO_4^{2-} + SO_3^- + H^+$	7.5×10^8
5a	$SO_5^- + SO_5^- \rightarrow SO_4^- + SO_4^- + O_2$	8.7×10^7
5b	$SO_5^- + SO_5^- \rightarrow S_2O_8^{2-} + O_2$	1.3×10^7
6	$HSO_5^- + HSO_3^- + H^+ \rightarrow 2SO_4^{2-} + 3H^+$	**10^7
7	$Fe^{2+} + SO_5^- \xrightarrow{H^+} Fe^{3+} + HSO_5^-$	3.2×10^6
8	$Fe^{2+} + SO_4^- \rightarrow Fe^{3+} + SO_4^{2-}$	3.0×10^8
9	$Fe^{2+} + HSO_5^- \rightarrow Fe^{3+} + SO_4^- + OH^-$	3.5×10^4
10	$Mn^{2+} + SO_5^- \xrightarrow{H^+} ***Mn(III) + HSO_5^-$	10^8
11a	$Mn(III) + ****SO_{2(aq)} \rightarrow Mn^{2+} + SO_3^- + H_2O + H^+$	$\approx 3 \times 10^5$
11b	$Mn(III) + HSO_3^- \rightarrow Mn^{2+} + SO_3^- + H_2O$	$\approx 10^6$
12	$Mn(III) + SO_5^- \xrightarrow{H^+} Mn(IV) + HSO_5^-$	$\approx 10^8$
13	$Mn(III) + Mn(III) \rightarrow Mn^{2+} + Mn(IV)$	$\approx 10^5$
14	$Mn^{2+} + HSO_5^- \rightarrow Mn(III) + SO_4^-$	≈ 15
15	$Mn^{2+} + SO_4^- \rightarrow Mn(III) + SO_4^{2-}$	2×10^7

* First order rate constant.

** Third order rate constant.

*** $MnOH^{2+}$.

**** H_2SO_3.

Influence of Other Transition Metals

The discussed contradictions between catalytic reactivity of Mn/Fe ions according to monitoring data on the oxidation depth by $\Delta^{34}S$ and results of studying the reaction kinetic in bulk conditions were successfully removed in (Harris et al., 2013) by involving catalytic reactions of SO_2 oxidation with the participation of ions of other TMs detected in cloud droplets (Cu^{2+}, Ni^{2+}, Zn^{2+}, Ti, V, and Cr). In this way, up to ~60% of sulfur dioxide oxidated in the cloud were "bound." For the rate of the catalytic process with the participation of these TM ions, we have $w_{TM} = 0.6 \, w_{S(VI)\_atm.\_aq} \approx 4 \times 10^{-5}$ mol L^{-1} s^{-1}. Hence, for the observed process rate constant, we find $k_{obs} = w_{TM}/[HSO_3^-] \approx 400$ s^{-1}; for the squared sum of multiplied concentrations of TM ions in the expression for w_{TM}, we have $(\Sigma[TM])^2 = k_{obs}/(3.7 \times 10^7(10^{-pH})^{-0.74}) \approx 2 \times 10^{-8}$ mol^2/L^2. Taking into account the droplet phase content on large particles (Harris et al., 2013) and the quantity $(\Sigma[TM])^2$ we found, we come to the conclusion that the total TM content in the atmosphere exceeds their analytical value (≈ 6 ng/m^3) by two orders of magnitude. Note that the estimates of $(\Sigma[TM])^2$ involved the value of k_{Mn_Fe} at $T = 298$ K. At $T = 280$ K, which corresponds to conditions of field experiments, the value of this rate constant becomes lower almost by an order of magnitude. The use of the expression for w_{Mn_Fe} in calculations of w_{TM} also raises doubts. In this regard, we note that the observed catalysis of oxidation of sulfur dioxide solutions by Ni(II) and V(II) ions, e.g., according to data of (Brandt and Elding, 1998), is fully caused by contamination of nickel and vanadium preparations by iron impurities. The effect of added copper ions in this reaction manifests itself to an important degree only in far fewer acid solutions (pH 6)

(Grgić et al., 1991). As for catalysis by Cr ions at the considered values of pH ($\approx$3.8), it is also impossible (Brandt and Elding, 1998).

The Effect of Enhancement of the Pairwise Action of Mn/Fe Ions

What is the real reason for the considered discrepancy between data of field experiments on the dynamics of the conversion $SO_2 \to SO_4^{2-}$ in $\Delta^{34}S$ and results of experiments on kinetics of the catalytic reaction with the participation of Mn/Fe ions in bulk conditions (Ibusuki and Takeuchi, 1987; Martin and Good, 1991)? It is a lack of knowledge about the mechanism of the catalytic action of the pair of these ions and, as a result, the incorrect use of the expression taken from the literature (Ibusuki and Takeuchi, 1987) for w_{Mn_Fe} in calculations of the SO_2 oxidation rate in the droplet phase of the cloud. Our consideration of the action mechanism of these metal ions shows that the effect of enhancement of their pairwise action (synergism) is related to enhancement of the catalytic action of iron ions by manganese ions (Ermakov and Purmal, 2002; Eremina et al., 2017). The apparent activity of manganese ions, which are not active in themselves (Ermakov and Purmal, 2002), is caused by acceleration of slow stages of the chain continuation (3a, 3b; see Table 1), as well as by the shift of the distribution of impurity iron ions with respect to the charge forms ([Fe(III)]/[Fe(II)]) for the catalytically active form Fe(III)—the *participant* of the reaction initiation (see reaction (1) in Table 1).

In (Ermakov and Purmal, 2002; Eremina et al., 2017), in the framework of the mechanism of the catalytic process with the participation of Mn/Fe ions presented in Table 1, a quantitative agreement was successively achieved for almost all available experimental data on the physical modeling of catalytic oxidation of sulfur dioxide in bulk experiments in the presence of iron and manganese ions. However, the results of new experiments on laboratory modeling of the dynamics of the catalytic reaction in deliquesced aerosol particles remained unexplainable. The experiments were carried out in smog chambers and pointed to anomalously high $W_{S(VI)\_atm.}$ (Wang et al., 2016; Liu et al, 2020; Zhang et al., 2021). An important feature of these experiments is the large excess of manganese ions over the S(IV) content in droplets ($\alpha = [Mn^{2+}]/[S(IV)] \gg 1$). For example, in the investigations (Zhang et al., 2021), experiments for pH $\le$ 1.5 were carried out at $\alpha \approx 10^6$.

Branching Regime of Catalysis

Recently, in (Ermakov et al., 2023), we reported about a new (branching) regime of S(IV) oxidation catalysis by manganese ions. The regime is implemented in conditions of the excess of metal ions over S(IV). As it turned out, the decisive role in the dynamics of the process in this regime was played by chain branching with the participation of manganese ions and an intermediate product HSO_5^- generated in the course of the reaction (see reaction (14) in Table 1).

Instead of *one* active center HSO_5^- lost in the branching reaction, there appear two new chain carriers: Mn(III) and SO_4^-. The increase in their generation rate due to that is accompanied by an increase in the concentrations of chain carriers and HSO_5^- and, along with that, an increase in w_{Mn_Fe}. A parallel reaction $HSO_5^- + HSO_3^- + H^+ \to 2HSO_4^- + H^+$ (see reaction (6) in Table 1) competes with the consumption of HSO_5^- in the chain branching.

Under the predominance of the first one ($\alpha \gg 1$ and pH > 3), the process of SO_2 oxidation goes into the branching regime, which is accompanied by the experimentally observed (Wang et al., 2016; Liu et al, 2020; Zhang et al., 2021) rise in w_{Mn_Fe} with an increase in $[Mn^{2+}]$ and pH. On the contrary, under the predominant proceeding of reaction (6), i.e., under conditions of low α and small pH, branching of the chains $HSO_5^- + Mn^{2+}$ turns out to be suppressed. As a result, instead of the rise in w_{Mn_Fe}, a constancy of w_{Mn_Fe} with an increase in manganese ions is observed with an increase in (Mn^{2+}) observed in (Wang et al., 2016; Liu et al, 2020; Zhang et al., 2021) in experiments carried out in smog chambers and in bulk experiments at $\alpha \le 1$ and low pH ($\le$3) (Coughanowr and Krause, 1965; Berglund et al., 1993). Summarizing, we conclude that the transition of the catalytic reaction to the branching regime is regulated by the acidity of droplets and by the ratio of concentrations of Mn and S(IV) ions in them. The transition to the branching regime with an increase in pH requires lower and lower α (Ermakov et al., 2023), which is related to the decrease in the rate of the reaction $HSO_5^- + HSO_3^- + H^+$ with a decrease in acidity of droplets.

The Role of the Excess of Mn/Fe Ions

The preceding sheds light on causes of the rapid oxidation of sulfur dioxide in condensed moisture on the surface of large particles (Harris et al., 2013), despite its small volume fraction on these particles in the episode FCE-11.2. We recall that TM dissolution in moisture that coats the particles was considered in (Harris et al., 2013) as the only reason of catalytic SO_2 oxidation. The dissolution of TMs is undoubtedly necessary for the implementation of the catalytic reaction. However, using data about the dynamics of the catalytic reaction with the participation of Mn/Fe ions (Ibusuki and Takeuchi, 1987) allows one to associate
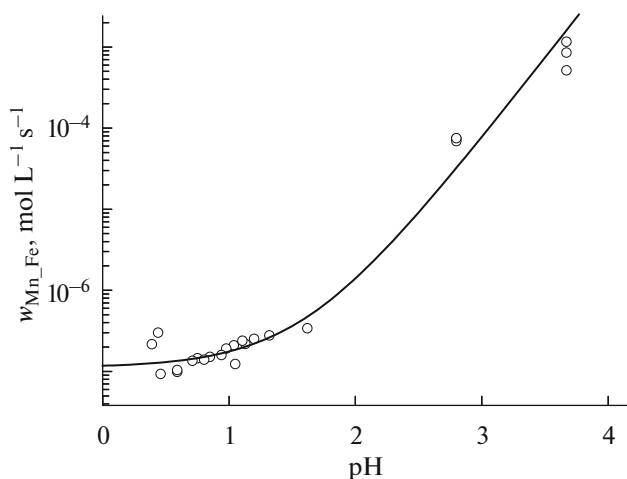
Fig. 2. Dependence of the rate w_{Mn_Fe} of sulfur dioxide oxidation on pH under common concentration conditions ($T = 298$ K, $\mu \approx 5$ mol/L, and $L \approx 3 \times 10^{-10}$ (≈ 300 µg/m³), $P_{SO_2} = 40$ ppb, and the concentration of manganese ions is 40 ng/m³) according to (Wang et al., 2016; Liu et al., 2020; Zhang et al., 2021); see the dots. The solid curve is the calculated data.

with this process not more than a few percent of the observed SO₂ conversion. In this regard, it was erroneously proposed to widen the circle of catalytic reactions with the participation of ions of other TMs that were also observed in large particles of coarsely dispersed mineral aerosol, although the data available in the literature do not corroborate these assumptions. Number concentrations of such particles and, as a result, the *low* content of condensed moisture on their surface (generally, its content in the cloud) turn out to be no less important than the dissolution of TMs contained in large particles of coarsely dispersed mineral aerosol. As a result, the concentration of manganese ions in droplets on these particles noticeably exceeds the concentration of S(IV) ($\alpha \gg 1$, see the dashed line *2** in Fig. 1). In combination with the not too low pH level in droplets (3.8), this excess of metal ions over S(IV) seemingly provides the transition of the reaction into the branching regime (Ermakov et al., 2023), which is accompanied by deep and rapid self-purification of air coming to the cloud from SO₂ in the episode FCE-11.2.

Role of Conditions of Catalytic Reaction Proceeding

As an illustration of the differences in the reaction dynamics when the catalytic reaction goes from the chain nonbranching regime into the branching regime, Fig. 2 shows the dependence of w_{Mn_Fe} on pH according to data of laboratory experiments with aerosol particles (Wang et al., 2016; Liu et al., 2020; Zhang et al., 2021) (see the dots). Calculations of w_{Mn_Fe} by data of different experiments (see the curve) were carried out with allowance for the recalculation of concentrations of manganese ions and S(IV) in particles to common concentration conditions ($T = 298$ K, $\mu \approx 5$ mol/L, the condensed moisture content of 100 and 300 µg/m³, pH 0–4, $P_{SO_2} = 40$ ppb, and [Mn²⁺] = 40 ng/m³), where μ is the ionic strength. It is seen that the experimental data in general follow the behavior of the calculated curve and point to correctness of the considered mechanism of the catalytic reaction in the branching regime. It follows from data of Fig. 2 that a close to saturation $w_{Mn\_Fe} \approx 10^{-7}$ mol L⁻¹ s⁻¹ is observed at pH < 1.5. Under these conditions, the catalytic reaction proceeds in the chain nonbranching regime (Ermakov et al., 2023), because the rate of reaction (6) exceeds manifold the rate of chain branching (14) (see Table 1). With a decrease in acidity of particles, w_{Mn_Fe} increases by several orders of magnitude. Such a pronounced influence of the decrease in acidity of the solutions on w_{Mn_Fe} is explained by suppression of the negative influence of reaction (6) and the transition of the reaction into the branching regime.

ON THE DYNAMICS OF SO₂ OXIDATION IN CLOUD DROPLETS

We meet attributes of SO₂ oxidation in the droplet phase in the branching regime in the real atmosphere when we consider monitoring data on the aerosol haze that envelops Beijing and other cities of southeast China in winter (Zheng et al., 2015; Cheng et al., 2016; Wang et al., 2016; Xie et al., 2019; Liu et al., 2020). The particle concentration level PM₂.₅ monitored every hour approaches ≈ 900 µg/m³ (Liu et al., 2020). At the same time, despite the low insolation and low concentrations of SO₂ oxidants in the atmosphere ($O_3 \leq 1$ ppb), as well as extremely low moisture content in the particles (100÷300 µg/m³), an unprecedently high rate of sulfate formation in haze particles is observed ($W_{S(VI)\_atm.} \sim$ tens of µg m⁻³ h⁻¹) (Wang et al., 2016; Liu et al, 2020; Zhang et al., 2021). Apparently, we meet a similar reaction regime in the episode FCE-11.2 in the HCCT-2010 campaign. This regime is implemented not in all droplets in the cloud, but only in their small fraction, including large particles of coarsely dispersed mineral aerosol as condensation nuclei.

As was pointed out above, the reaction rate we calculated using the empirical expression (Ibusuki and Takeuchi, 1987) at the condensed moisture content in the air (3.7×10^{-4} L/m³), $T \approx 280$ K, and pH ≈ 3.8 (≤ 4.2) is $w_{Mn\_Fe} \approx 3 \times 10^{-9}$ mol L⁻¹ s⁻¹. This value of the reaction rate is shown by dashed line *2* in Fig. 1. At the same time, it was noted in (Harris et al., 2013) that this value does not exceed 3% of the observed sulfur dioxide oxidation rate calculated by data on $\Delta^{34}S$ in sulfur dioxide. Hence, for the observed reaction rate we have $w^*_{Mn\_Fe\_obs} \approx 30\, w_{Mn\_Fe} \approx 2 \times 10^{-7}$ mol L⁻¹ s⁻¹ (see the

dashed line *2** in Fig. 1). Previously, in (Ermakov et al., 2023), we presented an analytical expression for the observed reaction rate constant in the branching regime $k_{Mn\_Fe}^*$. As applied to conditions of the field experiments under consideration, the numerical value of this rate constant is $k_{Mn\_Fe}^* = 7 \times 10^5 \, L \, mol^{-1} \, s^{-1}$. For the reaction rate in droplets in the branching regime (Ermakov et al., 2023), we finally find $w_{Mn\_Fe}^* \approx 2 \, k_{Mn\_Fe} [Mn^{2+}][HSO_3^-] \approx 2 \times 7 \times 10^5 \, 1.2 \times 10^{-6} \, 10^{-7} \approx 1.7 \times 10^{-7} \, mol \, L^{-1}$, which in essence reproduces the abovementioned value of $w_{Mn\_Fe\_obs}$. Here, 1.2×10^{-6} and 10^{-7} are the concentrations of manganese ions and S(IV), mol/L, respectively. Attention is attracted by the fact that the concentration of iron ions—a participant of initiation of reaction (1) (see Table 1)—is absent in the expression for $w_{Mn\_Fe}^*$. This fact means that iron ions in the branching regime manifest themselves only at the stage of generation of *primary* chain carriers (SO_3^-) (1) (see Table 1). However, the following increase in their concentration is fully determined by the dynamics of the chain branching reaction (14). The value of $w_{Mn\_Fe}^*$ that we found makes it possible to estimate the real coefficient of reactive SO_2 uptake by the droplet phase on the surface of large particles: $\gamma_{SO_2} = 4 w_{Mn\_Fe}^* N_a r / 3 \times 10^3 \, [SO_2] \, \varpi_{SO_2} \approx 3.2 \times 10^{-4}$, which agrees, e.g., with data (Pozzoli et al., 2008). Here, $10^3 \, cm^3/L$ is a dimension factor.

Within the framework of the proposed mechanism of the reaction, the nonparticipation of hydrogen peroxide in sulfate formation in condensed moisture on the surface of large particles becomes clear. The reason for this is the many times higher rate of the catalytic reaction in the branching regime as compared to that with the participation of hydrogen peroxide (by a factor of $\approx 10^2$); see dashed lines *2* and *2** in Fig. 1. The unexpressed role of the catalytic process in other nighttime episode FCE-7.1 also becomes clear. The investigations of (Harris et al., 2013) pointed to the significantly lower efficiency of large particle activation in this episode and a noticeably lower content of moisture in them, which apparently restrained the leaching of TM ions from particles. A natural explanation can be also found for the larger values of w_{Mn_Fe} in the droplet phase which are revealed in comparable concentration conditions as compared to those observed in bulk experiments enhanced sulfate formation. In (Angle et al., 2021), their difference was attributed to the formation of specific zones in the droplets ("surface effects and potentially aerosol pH gradients"). In (Lee et al., 2019), the generation of small quantities of hydrogen peroxide ($\approx 10^{-6}$ mol/L) during droplet spraying in laboratory conditions was discussed as the cause of this phenomenon. In (Hung et al., 2018), the acceleration of the catalytic reaction in droplets was associated with acceleration of the initiation process caused by the generation of SO_3^- radicals due to the surface reaction. The above is contrary to results of our data comparison in (Ermakov et al., 2023) about the reaction kinetics in bulk experiments [14], [15] and in small immobile droplets (Barrie and Georgii, 1976; Kaplan et al., 1981) at pH ≤ 3 and α < 250. It pointed to close $w_{S(VI)}$ in these experiments and, therefore, the identity of the mechanism of S(VI) formation at given pH and α.

In reality, the observed acceleration of the catalytic generation of sulfates in droplets as compared to bulk experiments under comparable conditions is caused by the closeness to constancy of the concentrations of components of dissolved SO_2 and the intermediate product HSO_5^- in droplets in the course of the reaction. In contrast to bulk experiments, the constancy of S(IV) concentration in aerosol particles sustains the rapid uptake of SO_2 from the gas (Wang et al.; 2016; Liu et al, 2020; Zhang et al., 2021). Owing to the high rate of chain branching, the concentration of the intermediate product HSO_5^- in droplets turns out to be much higher even than the level of [S(IV)] (Ermakov et al., 2023). The excess of the sulfur dioxide oxidation rate in the droplet phase as compared to bulk conditions is related just to the conjugation of these two physicochemical processes.

CONCLUSIONS

In this work, by means of the example of data on the dynamics of sulfur dioxide oxidation in an orographic cloud, the specificity of this process in the droplet phase in the presence of transition metal ions is considered. An analysis of these field data shows that the rapid experimentally observed oxidation of sulfur dioxide in cloud droplets is implemented mainly on deliquesced particles of coarsely dispersed mineral aerosol subjected to active leaching of Mn/Fe ions. The decisive role in rapid self-purification of the air coming to the cloud from SO_2 is played here by the transition of the catalytic reaction to the branching oxidation regime. Iron ions provide the initial initiation of the catalytic process and the reaction of chain branching with the participation of manganese ions and the intermediate product HSO_5^- leads to the appearance of two new chain carriers: Mn(III) and SO_4^-. The increase in the rate of their generation due to this is accompanied by an increase in concentrations of the chain carriers. In combination with the favorable level of acidity of condensed moisture on the surface of large particles of coarsely dispersed mineral aerosol, this provides the rapid oxidation of sulfur dioxide despite the extremely low volume fraction of the condensed moisture occupied by droplets on the surface of large particles in the cloud. Thus, droplets of different fractions in the cloud turn out to be unequal

for catalytic intracloud processes not only due to differences in their sizes. The results obtained in this work indicate the significance and potential abundance of catalytic processes of SO_2 oxidation in the global atmosphere and point to the necessity of taking them into account when considering the budget of sulfates in the atmosphere and their influence on the climate.

FUNDING

CONFLICT OF INTEREST

The authors declare that they have no conflicts of interest.

REFERENCES

Alexander, B., Park, R.J., Jacob, D.J., et al., Transition metal-catalyzed oxidation of atmospheric sulfur: global implications for the sulfur budget, *J. Geophys. Res.: Atmos.*, 2009, vol. 114, p. D02309.

Andreae, M.O., Jones, C.D., and Cox, P.M., Strong present-day cooling implies a hot future, *Nature*, 2005, vol. 435, no. 7046, pp. 1187–1190.

Angle, K.J., Neal, E.E., and Grassian, V.H., Enhanced rates of transition-metal-ion-catalyzed oxidation of S(IV) in aqueous aerosols: Insights into sulfate aerosol formation in the atmosphere, *Environ. Sci. Technol.*, 2021, vol. 55, no. 15, pp. 10291–10299.

Barrie, L.A. and Georgii, H.W., An experimental investigation of the absorption of sulphur dioxide by water drops containing heavy metal ions, *Atmos. Environ.*, 1976, vol. 10, no. 9, pp. 743–749.

Behra, P. and Sigg, L., Evidence for redox cycling of iron in atmospheric water droplets, *Nature*, 1990, vol. 344, no. 6265, pp. 419–421.

Berdnikov, V.M. and Bazhin, N.M., Redox potentials of some inorganic radicals in aqueous solutions, *Zh. Fiz. Khim.*, 1970, vol. 44, pp. 712–716.

Berglen, T., Berntsen, T., Isaksen, I., and Sundet, J., A global model of the coupled sulfur/oxidant chemistry in the troposphere: The sulfur cycle, *J. Geophys. Res.*, 2004, vol. 109, no. 19, p. D19310.

Berglund, J., Fronaeus, S., and Elding, L.I., Kinetics and mechanism for manganese-catalyzed oxidation of sulfur (IV) by oxygen in aqueous solution, *Inorg. Chem.*, 1993, vol. 32, no. 21, pp. 4527–4537.

Betterton, E.A. and Hoffman, M.R., Oxidation of aqueous SO_2 by peroxomonosulfate, *J. Phys. Chem.*, 1988, vol. 92, no. 21, pp. 5962–5965.

Brandt, Ch. and Elding, L.I., Role of chromium and vanadium in the atmospheric oxidation of sulfur(IV), *Atmos. Environ.*, 1998, vol. 32, no. 4, pp. 797–800.

Cheng, Y.F., Zheng, G., Way, Ch., and Mu, Q., Reactive nitrogen chemistry in aerosol water as a source of sulfate during haze events in China, *Sci. Adv.*, 2016, vol. 2, no. 12, p. e1601530.

Coughanowr, D.R. and Krause, F.E., The reaction of SO_2 and O_2 in aqueous solutions of $MnSO_4$, *Ind. Eng. Chem. Fund*, 1965, vol. 4, no. 1, pp. 61–66.

Eremina, I.D., Aloyan, A.E., Arutyunyan, V.O., Larin, I.K., Chubarova, N.E., and Ermakov, A.N., Hydrocarbonates in atmospheric precipitation of Moscow: Monitoring data and analysis, *Izv., Atmos. Ocean. Phys.*, 2017, vol. 53, no. 3, pp. 334–342.

Feichter, J., Kjellstrom, E., Rodhe, H., et al., Simulation of the tropospheric sulfur cycle in a global climate model, *Atmos. Environ.*, 1996, vol. 30, nos. 10–11, pp. 1693–1707.

Fomba, K.W., Muller, K., van Pinxteren, D., and Herrmann, H., Aerosol size-resolved trace metal composition in remote northern tropical Atlantic marine environment: Case study Cape Verde Islands, *Atmos. Chem. Phys. Discuss.*, 2013, vol. 13, no. 9, pp. 4801–4814.

Grell, G.A., Peckham, S., Schmitz, R., et al., Fully coupled "online" chemistry within the WRF model, *Atmos. Environ.*, 2005, vol. 39, no. 37, pp. 6957–6975.

Grgić, I., Hudnik, V., Bizjak, M., and Levec, J., Aqueous S(IV) oxidation. I. Catalytic effects of some metal ions, *Atmos. Environ.*, 1991, vol. 25A, no. 8, pp. 1591–1597.

Gröner, E. and Hoppe, P., Automated ion imaging with the nanoSIMS ion microprobe, *Appl. Surf. Sci.*, 2006, vol. 252, no. 19, pp. 7148–7151.

Harris, E., Sinha, B., Hoppe, P., et al., Sulfur isotope fractionation during oxidation of sulfur dioxide: Gas-phase oxidation by oh radicals and aqueous oxidation by H_2O_2, O_3 and iron catalysis, *Atmos. Chem. Phys.*, 2012a, vol. 12, no. 1, pp. 407–423.

Harris, E., Sinha, B., Foley, S., et al., Sulfur isotope fractionation during heterogeneous oxidation of SO_2 on mineral dust, *Atmos. Chem. Phys.*, 2012b, vol. 12, pp. 4867–4884.

Harris, E., Sinha, B., van Pinxteren, D., et al., Enhanced role of transition metal ion catalysis during in-cloud oxidation of SO_2, *Science*, 2013, vol. 340, no. 6133, pp. 727–730.

Herrmann, H., Ervens, B., Jacobi, H.-W., et al., Capram2.3: A chemical aqueous phase radical mechanism for tropospheric chemistry, *J. Atmos. Chem.*, 2000, vol. 36, pp. 231–284.

Hung, H.-M., Hsu, M.-N., and Hoffmann, M.R., Quantification of SO_2 oxidation on interfacial surfaces of acidic micro-droplets: Implication for ambient sulfate formation, *Environ. Sci. Technol.*, 2018, vol. 52, no. 16, pp. 9079–9086.

Ibusuki, T. and Takeuchi, K., Sulfur dioxide oxidation by oxygen catalyzed by mixtures of manganese(II) and iron(III) in aqueous solutions at environmental reaction conditions, *Atmos. Environ.*, 1987, vol. 21, no. 7, pp. 1555–1560.

Kaplan, D., Himmelblau, D.M., and Kanaoka, C., Oxidation of sulfur dioxide in aqueous ammonium sulfate aerosols containing manganese as a catalyst, *Atmos. Environ.*, 1981, vol. 15, no. 5, pp. 763–773.

Kulmala, M., Pirjola, U., and Mäkelä, U., Stable sulphate clusters as a source of new atmospheric particles, *Nature*, 2000, vol. 404, no. 6773, pp. 66–69.

Laj, P., Fuzzi, S., Facchini, M.C., et al., Cloud processing of soluble gases, *Atmos. Environ.*, 1997, vol. 31, no. 16, pp. 2589−2598.

Lee, J.K., Samanta, D., Nam, H.G., and Zare, R.N., Micrometer-sized water droplets induce spontaneous reduction, *J. Am. Chem. Soc.*, 2019, vol. 141, no. 27, pp. 10585−10589.

Liu, P., Ye, C., Xue, Ch, Zhang, Ch., Mu, Yu., and Sun, X., Formation mechanisms of atmospheric nitrate and sulfate during the winter haze pollution periods in Beijing: Gas-phase, heterogeneous and aqueous-phase chemistry, *Atmos. Chem. Phys.*, 2020, vol. 20, no. 7, pp. 4153−4165.

Liu, T., Clegg, S.L., and Abbatt, J.P.D., Fast oxidation of sulfur dioxide by hydrogen peroxide in deliquesced aerosol particles, *Proc. Natl. Acad. Sci. U. S. A.*, 2020, vol. 117, no. 3, pp. 1354−1359.

Martin, L.R. and Good, T.W., Catalyzed oxidation of sulfur dioxide in solution: the iron-manganese synergism, *Atmos. Environ.*, 1991, vol. 25A, no. 10, pp. 2395−2399.

Mauldin, R.L., Madronich, S., Flocke, S.J., et al., New insights on OH: Measurements around and in clouds, *Geophys. Res. Lett.*, 1997, vol. 24, no. 23, pp. 3033−3036.

McCabe, J.R., Savarino, J., Alexander, B., et al., Isotopic constraints on non-photochemical sulfate production in the arctic winter, *Geophys. Res. Lett.*, 2006, vol. 33, no. 5, p. L05810.

Pozzoli, L., Bey, I., Rast, S., Schultz, M.G., Stier, P., and Feichter, J., Trace gas and aerosol interactions in the fully coupled model of aerosol−chemistry−climate ECHAM5-HAMMOZ: 1. Model description and insights from the spring 2001 TRACE-P experiment, *J. Geophys. Res.*, 2008, vol. 113, p. D07308.

Sedlak, D.L., Hoigne, J., David, M.M., et al., The cloudwater chemistry of iron and copper at Great Dun Fell, U.K., *Atmos. Environ.*, 1997, vol. 31, no. 16, pp. 2515−2526.

Seinfeld, J.H. and Pandis, S.N., *Atmospheric Chemistry and Physics, from Air Pollution to Climate Change*, Hoboken, N.J.: John Wiley and Sons, 2016.

Tilgner, A., Bräuer, P., Wolke, R., and Herrmann, H., Modelling multiphase chemistry in deliquescent aerosols and clouds using CAPRAM3.0i, *J. Atmos. Chem.*, 2013, vol. 70, no. 3, pp. 221−256.

van Eldik, R., Coichev, N., Reddy, K.B., and Gerhard, A., Metal ion catalyzed autoxidation of sulfur(IV) oxides: Redox cycling of metal ions induced by sulfite, *Ber. Bunsen-Ges. Phys. Chem.*, 1992, vol. 96, no. 3, pp. 478−481.

Wang, G.H., Zhang, R.Y., Gomes, M.E., et al., Persistent sulfate formation from London fog to Chinese haze, *Proc. Natl. Acad. Sci. USA*, 2016, vol. 113, no. 48, pp. 13630−13635.

Warneck, P., Mirabel, P., Salmon, G.A., et al., Review of the activities and achievements of the EUROTRAC subproject HALIPP, in *Heterogeneous and Liquid Phase Processes*, Warneck, P., Ed., Berlin: Springer, 1996, p. 7.

Winterholler, B., Hoppe, P., Foley, S., and Andreae, M.O., Sulfur isotope ratio measurements of individual sulfate particles by NanoSIMS, *Int. J. Mass Spectrom.*, 2008, vol. 272, no. 1, pp. 63−77.

Xie, Y.Z., Liu, Z.R., Wen, T.X., et al., Characteristics of chemical composition and seasonal variations of PM2.5 in Shijiazhuang, China: Impact of primary emissions and secondary formation, *Sci. Total Environ.*, 2019, vol. 677, pp. 215−229.

Yermakov, A.N., On the influence of ionic strength on the kinetics of sulfite oxidation in the presence of Mn(II), *Kinet. Catal.*, 2022, vol. 63, no. 2, pp. 157−165.

Yermakov, A.N. and Purmal, A.P., Catalysis of oxidation HSO_3^-/SO_3^{2-} by manganese ions, *Kinet. Catal.*, 2002, vol. 43, no. 2, pp. 249−260.

Yermakov, A.N., Aloyan, A.E., and Arutyunyan, V.O., Dynamics of sulfate origination in atmospheric haze, *Opt. Atmos. Okeana*, 2023, vol. 36, no. 2, pp. 148−153.

Zhang, H., Xu, Y., and Jia, L., A chamber study of catalytic oxidation of SO_2 by Mn^{2+}/Fe^{3+} in aerosol water, *Atmos. Environ.*, 2021, vol. 245, p. 118019.

Zheng, G.J., Duan, F.K., Su, H., et al., Exploring the severe winter haze in Beijing: The impact of synoptic weather, regional transport and heterogeneous reactions, *Atmos. Chem. Phys.*, 2015, vol. 15, no. 6, pp. 2969−2983.

Translated by A. Nikol'skii